Influence of Reduction Conditions on H_2 Adsorption in High-Surface Rh/CeO_2 Catalysts as Deduced by Volumetry, Calorimetry, and ^1H NMR Techniques

J. P. Belzunegui and J. Sanz*

Instituto de Ciencia de Materiales de Madrid, C.S.I.C., Campus Universitario de Cantoblanco, 28049 Madrid, Spain

José M. Guil

Instituto de Química Física "Rocasolano", C.S.I.C., C/Serrano 119, 28006 Madrid, Spain

Received: May 25, 2005; In Final Form: August 20, 2005

^1H NMR spectra corresponding to H_2 adsorption on high-surface Rh/CeO_2 catalysts ($S_{BET} \approx 55$ m^2/g) are formed by two lines, attributed to hydrogen adsorbed on ceria (resonance line A) and rhodium-metal particles (upfield-shifted line B). The evolution of ^1H NMR spectra as a function of temperature, time, and type of reduction (static or dynamic) allows the study of the progressive establishment of the strong metal-support interaction (SMSI) in Rh/CeO_2 catalysts. As the reduction progresses, the mean adsorption heat and the amount of hydrogen adsorbed on the metal, deduced from volumetry, NMR, and calorimetry techniques, decrease considerably. As a consequence of the decrease in metal activity, the amount of hydrogen transferred to the support CeO_2 is also reduced (spill-over processes). Outgassing of samples at 773 K eliminates hydrogen species retained at the metal−support surface, and oxidation treatments at 473 and 673 K eliminate the electronic effect and physical blocking of metal particles. The oxidation at 673 K recuperates the total adsorption capacity of metal particles. On the basis of these treatments, the contribution of different processes to the SMSI effect is analyzed. Electronic perturbation of rhodium particles is higher when reductions are performed in dynamic conditions; however, the importance of physical blocking of metal particles increases in static reductions. High reducibility of ceria strengthens electronic effects in Rh/CeO_2 compared to those observed in Rh/TiO_2 catalysts.

Introduction

Three-way catalysts (TWCs) are widely used for elimination of pollutants in automobile exhausts. They are formed by precious metals (Pt and Rh) dispersed on different supports (SiO_2, Al_2O_3, ...) to increase the metal surface exposed. In these catalysts, other additives such as cerium oxide have important roles as promoters. In recent years, the Rh/CeO_2 system has been extensively studied to understand the interaction mechanisms between rhodium metal particles and ceria.[1−2] Two main reasons explain the interest in this oxide: first, it works as a structural promoter, enhancing the metal dispersion and avoiding the metal sintering;[3] and second, it works as a chemical promoter, enhancing the oxygen storage capacity (OSC) of the catalyst. This ability is mainly the result of the easy Ce^{4+}/Ce^{3+} conversion in ceria oxide.[4]

The high-temperature reduction of Rh/TiO_2 and Rh/CeO_2 catalysts favors the interaction of the reduced support with supported metal particles, decreasing the capacity of metal particles to adsorb hydrogen (SMSI effect).[5,6] This effect was explained in Rh/TiO_2 in terms of (i) the hydride species,[7,8] formed at intermediate temperatures, and (ii) the electronic perturbation[9−16] or physical blocking[15−19] of metal particles, produced at high temperatures. Outgassing at 773 K produced an elimination of hydrides, but electronic and coverage effects were not affected by this treatment.[20,21] Oxidation at 473 K produced an elimination of electronic perturbation of metal particles.[22] Finally, the HRTEM analysis[15,16] of reduced samples showed that reduction of Rh/CeO_2 catalysts produced the migration of CeO_x moieties onto metal particles. In textural stabilized Rh/CeO_2 catalysts, reduction temperatures near 1173 K are needed to produce the CeO_x migration, and oxidation temperatures near 873 K required to restore the chemisorption capacity of the catalysts.[15,16] However, the ^1H NMR study of high-surface Rh/CeO_2 catalysts, showed that metal coverage can be produced at considerably lower temperatures, 773 K, and that the elimination of CeO_x species is produced during the oxidation at 673 K.[22]

In this work, we analyze the influence of different experimental conditions (time, temperature, and type of reduction) on the establishment of metal−support interactions (SMSI) in high-surface Rh/CeO_2 catalysts. In particular, the relative importance of electronic and coverage effects to the suppression of the metal adsorption capacity is studied with volumetry, calorimetry, and ^1H NMR techniques. For this purpose, the ^1H NMR technique, capable of differentiating hydrogen adsorbed on metal particles from that retained on the support, has been used. In this work, information deduced previously about metal coverage[22] will be used to determine the metal electronic perturbation produced by CeO_x species migrated onto the metal particles during reduction treatments.

Experimental Section

Samples. Incipient wetness impregnation of CeO_2 (rhodia, $S_{BET} = 109$ m^2g^{-1}) with an aqueous solution of $Rh(NO_3)_3$ salt

* To whom correspondence will be addressed.

10.1021/jp052766x CCC: $30.25
Published on Web 09/27/2005

was used to prepare Rh/CeO_2 catalyst with a final Rh loading of 2.5 wt %.[22,23] The S_{BET} of the Rh/CeO_2 catalysts reduced at 773 K and oxidized at 673 K decreased to 55 $m^2\ g^{-1}$. Metal dispersion determined by H_2 adsorption in the catalyst reduced at 473 K and outgassed at 523 K (H/Rh = 0.4), corresponds to particles with a mean size of 2,5 nm.[22]

Thermal treatments up to 773 K were carried out by placing 1 g of Rh/CeO_2 catalyst in Pyrex tubular cells provided with high-vacuum stopcocks. These cells allow the flow of gases through the catalyst as well as the outgassing of the sample. Reduction treatments at different temperatures and times were performed in conditions called "static" (closed cell with H_2 pressure of 150 Torr) or "dynamic" (H_2 flowing through the catalyst at ca. atmospheric pressure). Oxidation of the catalyst was always carried out under dynamic conditions.

Experimental Techniques. A heat flow microcalorimeter of the Tian−Calvet type (model BT, Setaram) was used to determine the differential heats of adsorption at 298 K. For this purpose, the calorimeter cells form part of a conventional volumetric apparatus, which allows the simultaneous determination of volumetric and calorimetric measurements. A capacitance manometer (Baratron 310, MKS) was used. Dead volumes were carefully calibrated either by mercury weighing or by helium expansions. Reproducibility of amounts adsorbed were always better than 0.2 μmol. The limit of detection of the microcalorimeter is about 0.2 mJ or 2 μW. The correction for the heat evolved in gas compression was previously determined with helium.

^{1}H NMR spectra were recorded at room temperature using a SXP 4/100 Bruker pulse spectrometer with an Aspect 2000 Fourier transform unit. The NMR frequency used for the proton signal was 75 MHz. Spectra were taken after $\pi/2$ pulse excitations (3.5 μs). The interval between successive accumulations (1 s) was chosen to avoid saturation effects. The number of accumulations (1000) was selected to obtain an apropriate signal-to-noise ratio ($S/N > 20$). Positions of NMR components are given relative to TMS (Me_4Si), with errors lower than 1 ppm. The intensities of the NMR lines were determined by comparing the integrated intensities with that of a known mica specimen.

Results

Volumetric isotherms corresponding to hydrogen adsorption on Rh/CeO_2 reduced at 373 K and outgassed at 423 K (14 h) are given in the top of Figure 1. A first isotherm (curve a) was measured; after that, the sample was outgassed at room temperature for 15 min, and a second isotherm (curve b) was obtained. Isotherm a shows an important increase at very low pressures, a clear knee, and a small increase that becomes almost linear in its final part. A total of 200 μmol H/g of catalyst was adsorbed at 75 Torr. The shape of isotherm b is similar to that of isotherm a, but the amount of hydrogen adsorbed at low pressures is appreciably smaller, 40 μmol H/g of catalyst. The hydrogen retained in the outgassed sample (160 μmol H/g of catalyst) was estimated by subtraction of two isotherms.

When the sample is reduced at 673 K and outgassed (14 h) at 673 K, an important decrease of the first part of the isotherm (curve c) is produced. The knee and the final part are similar to those of isotherms a and b, but the amount of hydrogen retained at 75 Torr is appreciably lower, 20 μmol H/g of catalyst. The readsorption isotherm measured in the outgassed sample (d) shows a similar slope, but the amount of hydrogen adsorbed is 10 μmol H/g of catalyst. This means that only 10 μmol H/g of catalyst is retained in the outgasssed sample. After the Rh/CeO_2 sample was reduced at 773 K, no adsorption was detected.

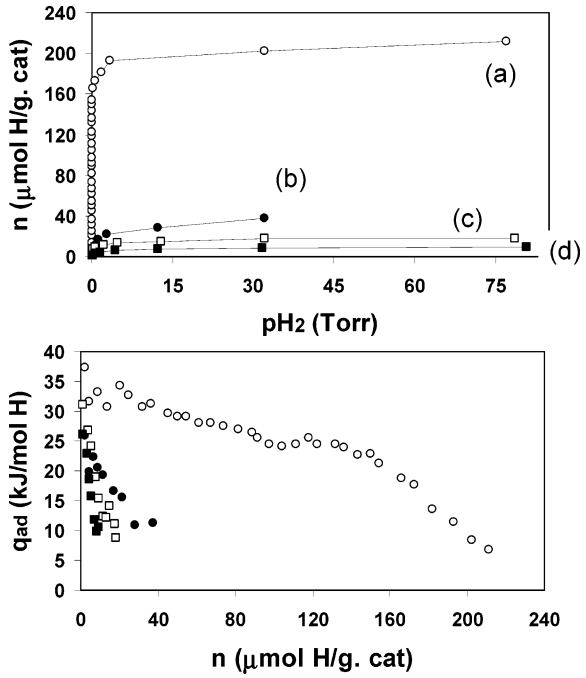

Figure 1. Hydrogen adsorption isotherms at room temperature on the Rh/CeO_2 sample: curve a (○), adsorption after H_2 reduction at 373 K and outgassing at 673 K (14h); curve b (●), readsorption after outgassing at room temperature; curves c (□) and d (■), similar experiments after H_2 reduction and outgassing at 673 K (top). Differential heats measured in H_2 adsorption and readsorption experiments described previously (bottom).

Differential adsorption heats (q_{ad}), corresponding to successive doses, are given as a function of the amount of hydrogen adsorbed (n) in the botton of the Figure 1 for the sample reduced at 373 K. A first decrease of q_{ad} from 37 to 30 kJ/mol of H is observed as n reaches 40 μmol H/g of catalyst. This value is similar to that reported in $Rh/SrTiO_3$ and Rh/TiO_2 catalysts for low-hydrogen coverages. After this, a second decrease from 30 to 25 kJ/mol of H was observed in the range of 40−100 μmol H/g of catalyst. Then, a plateau at 22 kJ/mol of H was detected between 100 and 140 μmol H/g of catalyst; finally, an important decrease of q_{ad} from 22 to 5 kJ/mol occurs in the range of 140−210 μmol H/g of catalyst. Readsorption only recovers the final part of the q_{ad} curve. In the samples reduced at 673 K, an important decrease in the amount of adsorbed hydrogen was detected in the Rh/CeO_2 catalyst. In this sample, a decrease from 32 to 10 kJ/mol of H was detected in the calorimetry plot. In the sample outgassed at 300 K, calorimetry data decrease from 26 to 10 kJ/mol of H. Values near 10 kJ/mol of H were measured in CeO_2 samples (data not given).

Figure 2 shows ^{1}H NMR spectra of the Rh/CeO_2 sample reduced in flowing H_2 at increasing temperatures, outgassed at 423 K(left) or 773 K(right), and exposed to H_2 (35 Torr) at room temperature. Two lines are observed: line A, centered at the resonance frequency, assigned to hydroxyl groups of the ceria support, and line B, shifted upfield, ascribed to hydrogen adsorbed on rhodium particles.[24] Hydrogen adsorbed on the metal particles was directly deduced from the I_B values; however, hydrogen adsorbed on the support was deduced from the $I_A - I_{A0}$ differences, where I_{A0} stands for intensity values in outgassed samples. Hydrogen adsorption deduced from I_A and I_B NMR intensities basically agrees with that determined by volumetric techniques.

Taking into account the fact that the intensity and position of line B depend on the H_2 pressure and the reduction extent of

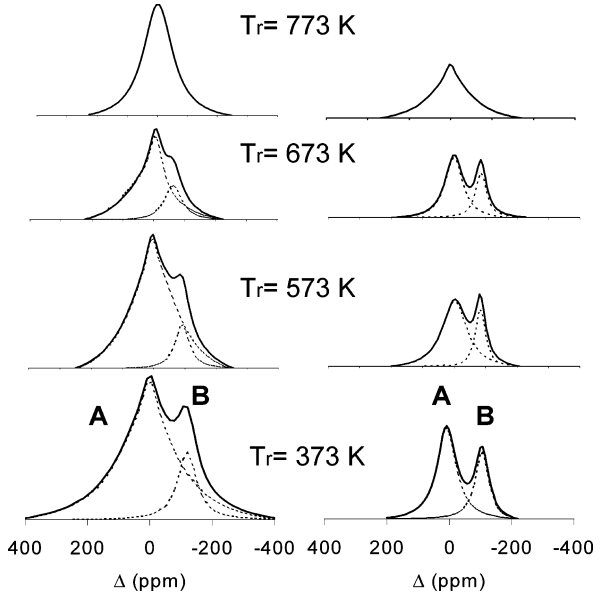

Figure 2. ^{1}H NMR spectra of the Rh/CeO_2 sample reduced under flowing H_2 (dynamic reduction) at the indicated temperatures. After the samples were outgassed at 423 K (left) or 773 K (right), they were exposed to H_2 (35 Torr) at room temperature before the NMR spectra were recorded.

the support,[24] we always recorded the NMR spectra on samples exposed to the same H_2 pressure (35 Torr). This pressure was chosen because the high amount of hydrogen adsorbed on metal particles and the high sensitivity of the position of line B to reduction treatments. When the sample is reduced at increasing temperatures and outgassed at 423 K (left) before H_2 adsorption, the intensity of both lines decreases progressively, as well as the chemical shift of line B. When the sample reduced at the indicated temperatures is outgassed at 773 K (right), the intensity values for line A were lower than those in the sample outgassed at 423 K, but the intensity and chemical shift of line B increased. In both cases, line B disappears from the NMR spectrum (SMSI state) when the sample was reduced at 773 K.

The evolution of the intensity (I_B) and the position (Δ) of line B versus reduction temperature in samples reduced in static and dynamic conditions are shown in Figure 3 (closed symbols). In all cases, I_B decreases with reduction temperature in the range of 373−773 K, indicating the progressive establishment of the SMSI state. The parallel decrease of Δ in the same range of temperature illustrates the progressive modification of the hydrogen−rhodium interaction in reduced samples. The variation of both parameters is more important in samples reduced in dynamic than in static conditions. In fact, reduction at 773 K in static conditions reduces the intensity of line B, while reduction of the sample in dynamic conditions produces the elimination of this line. The intensity of line A decreases with the temperature of reduction, indicating a partial dehydroxylation of the CeO_2 surface. The dehydroxylation is more pronounced in samples reduced in dynamic conditions (Figure 4).

Outgassing at 773 K (open symbols) of samples reduced in the range of 373−773 K, only partially recover I_B and Δ values (Figure 3). In the case of the sample reduced in dynamic conditions at 773 K, the outgassing of the sample at 773 K does not recover line B in adsorption experiments. In samples outgassed at 773 K, a considerable decrease on the line A was detected, corresponding to an important dehydroxylation of the support (Figure 4).

To analyze the irreversible loss of hydrogen adsorption on metal particles, I_B and Δ were studied as a function of reduction

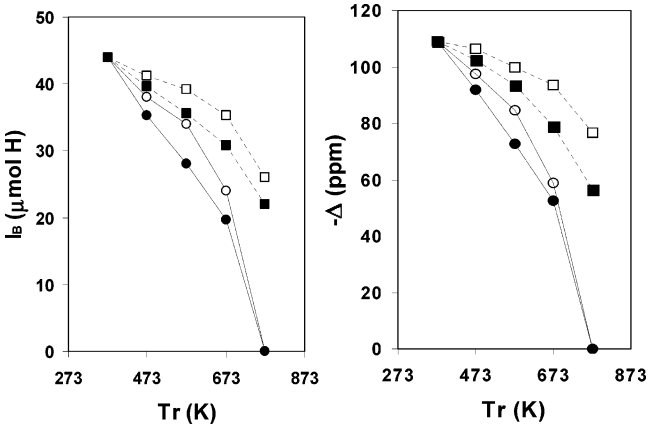

Figure 3. Intensity (I_B) and position ($\triangle$) of line B vs reduction temperature. Rh/CeO_2 catalysts were reduced in an accumulative process at increasing temperatures in dynamic (●) or static conditions (■). Reduction treatments at each temperature were carried out for 1 h. Samples outgassed at 773 K after reduction treatments are labeled with ○ and □. In all cases, I_B and Δ values were measured after outgassing at 423 or 773 K and exposition of the sample at room temperature to $p(H_2) = 35$ Torr.

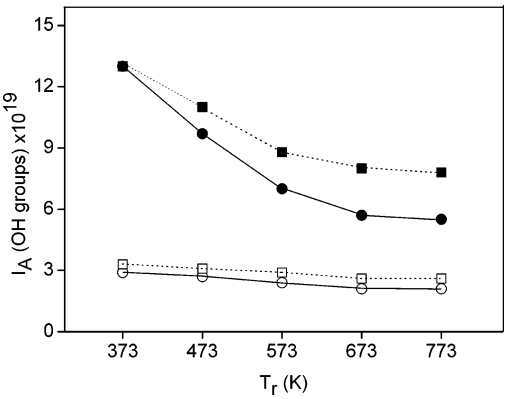

Figure 4. Intensity (I_A) of line A vs reduction temperature in dynamic (●) or static conditions (■). Reduction treatments at each temperature were carried out for 1 h. Samples outgassed at 773 K after reduction treatments are labeled with ○ and □.

time for different temperatures and type of treatment (Figure 5). In each experiment, the Rh/CeO_2 sample was reduced at 673 or 773 K for increasing times, outgassed at 773 K to eliminate hydrogen incorporated and finally exposed to H_2 (35 Torr) at room temperature. It was observed that I_B and Δ decrease for increasing reduction times, but the decrease in both parameters is higher in samples reduced in dynamic conditions.

Discussion

Volumetric data corresponding to samples reduced at 373 K show an important amount of hydrogen strongly absorbed at room temperature, 160 μmol H/g of catalyst, that is not eliminated by outgassing at 300 K. According to previous studies, this hydrogen corresponds to that retained onto the ceria support[24] and the metal particles.[25] Hydrogen readsorbed on the sample outgassed at 300 K corresponds to hydrogen weakly adsorbed on metal particles and to hydrogen reversibly spilt-over the ceria surface. Volumetric data show a big decrease in chemisorption, 20 μmol H/g of catalyst, when the sample is reduced at 673 K, and a lack of adsorption when the sample is reduced at 773 K (SMSI establishment).

The interpretation of volumetric data is not easy because hydrogen can be adsorbed simultaneouly on the metal and on

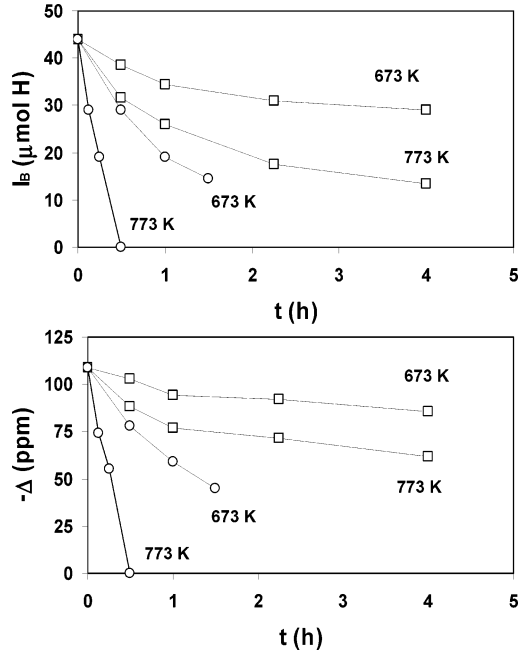

Figure 5. Effect of reduction time on intensity (I_B) and position (△) of line B for different reduction treatments. Rh/CeO_2 samples were reduced at 673 and 773 K for increasing times in static (□) or dynamic (○) conditions. After reduction treatments samples were outgassed at 773 K and exposed to H_2 (35 Torr) at room temperature.

the support, and in both cases, hydrogen can be reversibly and irreversibly retained after outgassing treatments. A differentiation of hydrogen adsorbed on metal particles and on the ceria support has been obtained with ^1H NMR spectroscopy. The analysis of the ^1H NMR spectra of the samples reduced at 373 K and outgassed at 423 K, showed that the amount of hydrogen adsorbed on the support was 160 μmol H/g of catalyst and that adsorbed on metal particles was 40 μmol H/g of catalyst. This observation suggests that spill-over processes are important in Rh/CeO_2 catalysts oxidized at 673 K and reduced at low temperatures.

Two different processes can be produced at the metal−support interface, during reduction at increasing temperatures of Rh/CeO_2 catalysts: (1) hydrogen incorporation which produces reduction of Ce^{4+} cations and formation of OH groups [7,8,26−28] and (2) oxygen elimination from CeO_2 that increases the amount of vacancies at the CeO_2 surface.[10,12,19,28] The analysis of samples reduced in static and dynamic conditions and outgassed at 423 K shows that incorporation of hydrogen is comparable to dehydroxylation processes. In both processes, I_A only decreases 35% when the reduction temperature increases from 373 to 773 K. The importance of dehydroxylation increases during the dynamic reduction of samples and during the outgassing of samples at 773 K (Figure 4). Formation of vacancies at the metal−support interface favors, according to reactions 2 or 3, the incorporation of hydride-like species or the formation of Rh−Ce bonds

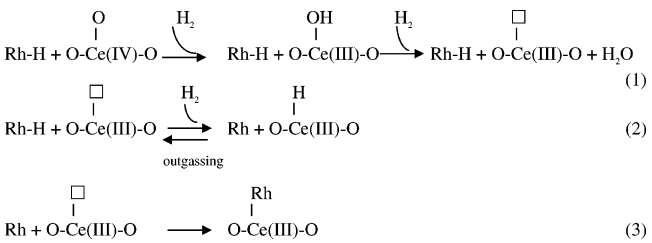

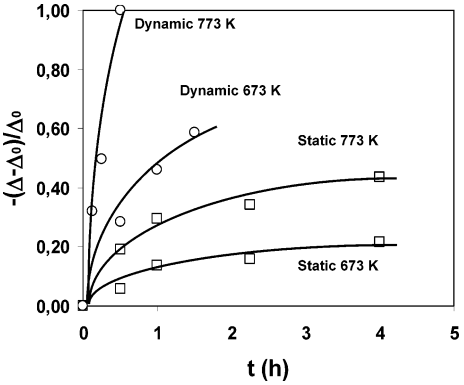

Figure 6. Plot of the electronic perturbation of metal particles $-(\Delta - \Delta_0)/\Delta_0$ vs reduction time in samples reduced in static and dynamic conditions at 673 and 773 K. The electronic perturbation was deduced by subtracting the position of line B in samples reduced at a given temperature (Δ) and oxidized at 473 K (Δ_0). These values were normalized with respect to $\Delta_0 = -109$ ppm. All measurements were carried out in samples exposed to $p(H_2) = 35$ Torr.

During the reduction process, the electronic perturbation of metal particles, produced by hydride species[7,8] and Rh−Ce bondings,[9−16] and the physical blocking of metal adsorption sites by CeO_x[17−19,22] species, are responsible for the observed decrease in the adsorption capacity of the metal particles (SMSI establishement).

The influence of temperature, time, and type of reduction on suppression of hydrogen adsorption on metal particles is analyzed in Figures 2, 3, and 5. It is observed that SMSI is produced in a progressive way; however, the hydrogen chemisorption loss is more important in samples reduced in dynamic than in static conditions. The outgassing of the sample at 773 K eliminates hydride-like species, but it does not affect physical blocking or electronic perturbation of metal particles.[20,21] From this fact, an estimation of the influence of hydride-like species in SMSI process can be deduced from the comparison of intensity of line B in samples reduced at increasing temperatures and outgassed at 773 K. This analysis shows that the influence of hydride-like species is not important and other effects are more determinant in SMSI establishment (Figure 3).

Oxidation at 473 K eliminates electronic perturbation but does not affect metal coverage requiring oxidation at 673 K for elimination of migrated CeO_x species. On the basis of this fact, the surface blocked by CeO_x species (θ) was estimated in a previous work, by comparing the intensity of line B in samples oxidized at 473 and 673 K, after each reduction treatment.[22] It was observed that θ increases with (i) the reduction temperature and (ii) the reduction time (quickly for short times and slowly for times higher than 1 h). However, θ was not appreciably affected by the type of reduction (static or dynamic).[22]

On the other hand, changes produced on the position of line B during reduction treatments are mainly associated with modifications produced on electronic properties of metal particles.[21] If the fact that the electronic perturbation of the metal is eliminated when samples are oxidized at 473 K ($\Delta_0 = -109$ ppm)[22] is taken into account, the difference between the chemical shift of line B of samples subjected to reduction treatments (Δ) and oxidized at 473 K (Δ_0) can be used here to estimate the electronic perturbation of the metal produced during reduction treatments. In this analysis, $-(\Delta - \Delta_0)$ values were normalized to that of the sample oxidized at 473K, $\Delta_0 = -109$ ppm. It is observed that $-(\Delta - \Delta_0)/\Delta_0$ increases with reduction time (Figure 6); however, the variation is more important (i) for higher reduction temperatures and (ii) when reductions are

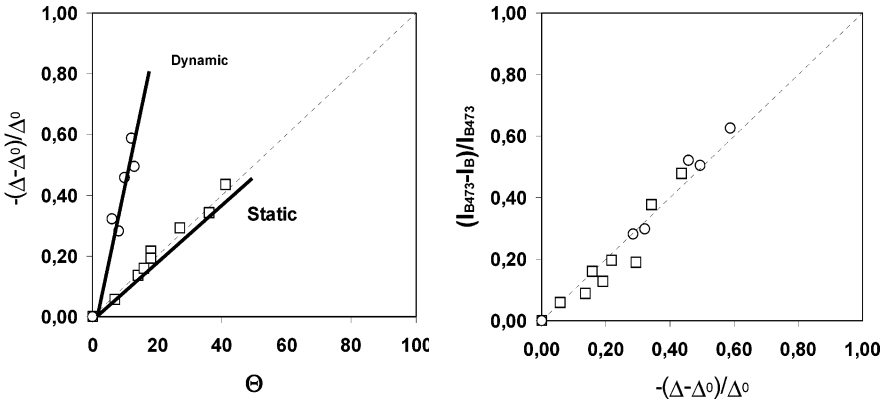

Figure 7. Plot of electronic perturbation, $-(\Delta - \Delta_0)/\Delta_0$, as a function of physical blocking, θ (left). Dependence of the chemisorption loss on electronic metal perturbation (right). In the last case, chemisorption losses were calculated with respect to those of the samples oxidized at 473 K (I_{B473}), in which blocking effects were not eliminated. Squares and circles correspond to samples reduced at 673 and 773 K in static and dynamic conditions (Table 1). Positions and intensity values of line B were measured at $p(H_2) = 35$ Torr.

carried out under dynamic conditions. Finally, it can be observed that adsorption capacity is more affected, for a given reduction temperature, by the electronic perturbation than by the physical blocking of metal particles (top of Figure 5). Similar results were obtained in calorimetry experiments. In this case, the reduction at 673 K, produced not only the decrease of differential adsorption heats but an important decrease of hydrogen adsorbed on the Rh/CeO_2 catalysts (Figure 1). In samples reduced at 673 K, a small amount of strongly adsorbed hydrogen was still produced, which has been ascribed to that adsorbed at metal steps, corners, and defects that are less afected by the electronic perturbation of metal particles.This adsorption was finally eliminated by reduction of Rh/CeO_2 at 773 K.

In the case of samples reduced in static conditions, the variation of $-(\Delta - \Delta_0)/\Delta_0$ values versus the reduction time displays a trend similar to that displayed by the θ parameter.[22] To ascertain whether electronic perturbation of the metal is associated with the migration of CeO_x species onto metal particles, the parameter $-(\Delta - \Delta_0)/\Delta_0$ was plotted versus θ in Figure 7 (left part). In all cases, electronic perturbation of the metal increases in a linear way with the extent of the metal surface covered by the CeO_x species; however, the increase of $-(\Delta - \Delta_0)/\Delta_0$ is more significant for dynamic treatments than it is for static reduction treatments. As an example, the dynamic reduction at 673 K for 90 min and the static reduction at 673 K during 60 min produce similar metal coverage (ca. 12−14%), but the electronic perturbation of the metal is much higher when reduction is carried out under dynamic conditions (55% vs 8%).

From the above results, it is clear that metal electronic perturbation is associated with coverage of metal particles by CeO_x species, but the detection of two different slopes in Figure 7 (left part) indicates that electronic perturbation of the metal changes considerably with the type of reduction used (static or dynamic). According to this fact, Figure 2 shows that the reduction at 773 K in dynamic conditions produces the total chemisorption loss, but reduction in static conditions only produces the partial decrease of signal B. These differences can be understood by assuming that during dynamic reductions the hydrogen flow pulls out the water molecules produced in reaction 1, favoring the formation of a higher amount of vacancies. As indicated previously, the formation of vacancies favors the creation of Rh−Ce bonds, which enhance the electronic perturbation of metal particles. However, the formation of vacancies at the CeO_2 surface seems to have a limited influence on the migration of CeO_x moieties on the metal particles.[22]

On the other hand, a deeper analysis of the chemisorption loss produced by electronic perturbation of the metal is given in Figure 7 (right). In this plot, we have not considered the contribution of the physical blocking to the metal adsorption capacity loss. For that, the new parameter used has been calculated by subtracting the line B intensity obtained for a given reduction treatment (I_B), from that measured in the sample oxidized at 473 K (I_{B473}) in which coverage was not eliminated. Finally, calculated differences were referred to the metal surface not affected by electronic perturbation (i.e., to the line B intensity of the sample oxidized at 473 K after each reduction treatment, I_{B473}). In this case, a good linear dependence between both parameters, $(I_{B473} - I_B)/I_{B473}$ and $-(\Delta - \Delta_0)/(\Delta_0)$, was obtained in samples reduced in static or dynamic conditions (Figure 7). From these results, it can be concluded that despite the reduction type, the parameter used, $(I_{B473} - I_B)/I_{B473}$, takes into account, selectively, the electronic perturbation produced in reduction treatments.

On the basis of the above considerations, it can be affirmed that electronic perturbation and physical blocking contribute to the hydrogen adsorption loss, but they are not strictly correlated (Figure 7, left). If it is assumed that the metal adsorption loss is the result of the sum of both effects, the relative contribution of physical blocking and electronic perturbation can be estimated in a separated way (Table 1). In general, both contributions increase with time and temperature of reduction, but electronic perturbation is favored in dynamic reductions and the physical blocking of metal particles is enhanced in static conditions.

At this point, it is interesting to compare results obtained in Rh/TiO_2[21,29] and Rh/CeO_2 catalysts, displaying a similar specific area ($S_{BET} \approx 50$ m^2 g^{-1}) (Table 1). In general, it is observed that for a fixed treatment (reduction time and temperature), the electronic perturbation produced is more important in Rh/CeO_2 than in Rh/TiO_2. Electronic perturbation is preponderant in Rh/CeO_2 reduced in dynamic conditions at 673 K, while physical blocking is more important in Rh/TiO_2 reduced in the same conditions. In both catalysts, dynamic reductions at 773 K produce an important electronic perturbation of metal particles. On the other hand, the static reduction of Rh/CeO_2 at 673 K for 135 min produces a percentage of physical blocking similar to the percentage of electronic effect (16−14%), but static reduction of Rh/TiO_2 at 723 K for 135 min produces more physical blocking than electronic effect (25−8%). A similar result is obtained in static reductions at 773 K.

Metal coverage is higher in Rh/TiO_2 than in Rh/CeO_2 for the same treatment (60% vs 40% in samples reduced in static

TABLE 1: Chemisorption Losses Produced by Physical Blocking and Electronic Perturbation of Rhodium Particles in High-Surface Rh/CeO_2 and Rh/TiO_2 Catalysts Submitted to Static and Dynamic Reductions[a]

		Rh/CeO_2			Rh/TiO_2[a]			
reduction type	T_r (K)	time (min)	physical blocking (%)	electronic effect (%)	T_r[a] (K)	time (min)	physical blocking (%)	electronic effect (%)
static	673	30	7	6	723	60	13	7
		60	14	8		135	25	8
		135	16	14		375	42	9
		240	18	16		735	48	19
static	773	30	18	10	773	15	8	4
		60	27	14		30	15	6
		135	36	24		90	27	15
		240	41	28		240	45	19
						330	53	18
						510	58	26
dynamic	673	30	8	26	723	30	8	8
		60	10	47		60	14	11
		90	12	55		90	20	17
dynamic	773	7.5	6	28	773	7.5	5	27
		15	13	47		12	8	55
		30	17	83		30	13	87

[a] Chemisorption values corresponding to the Rh/TiO_2 catalyst were taken from ref 21.

conditions at 773 K), but the time required to reach the plateau in θ versus t plots is smaller in Rh/CeO_2 (4 h) than in Rh/TiO_2 (9 h). The observed differences can been explained by considering the different reducibility of the two oxides. In the case of the more reducible CeO_2 oxide, reduction of the surface is produced in shorter times than that required for the reduction of TiO_2, but the migration of CeO_x is not favorable. In the case of TiO_2 oxide, reduction of the surface requires higher temperatures but migration of TiO_x is favored (Table 1). This explains why the metal coverage detected in Rh/TiO_2 is higher than that in Rh/CeO_2 catalysts. In each case, physical blocking of the metal by migrating CeO_x species depends only on the temperature and reduction time. However, dynamic reductions produce a higher amount of vacancies (reaction 1), and electronic effects are more intense.

In Rh/CeO_2 catalysts with a lower specific area ($S_{BET} \approx 10$ m^2 g^{-1}), the surface reduction is less important and the establishment of the SMSI behavior is shifted toward higher temperatures.[9,12,15,16] In these samples, the electronic perturbation at 773 K is preponderant because the metal coverage was delayed to temperatures higher than 973 K. On the basis of these facts, we can conclude that the behavior of metal-supported catalysts depends not only on the oxide reducibility but also on textural characteristics (specific surface area) of the support.

Conclusions

The detection of two components in the ^1H NMR spectra of Rh/CeO_2 catalysts, allowed the differentiation of hydrogen adsorbed on the metal from that adsorbed on the support. Hydrogen adsorption on metal particles decreases when the reduction temperature increases. In samples reduced at 773 K in dynamic conditions, hydrogen adsorption is eliminated, requiring an oxidation at 673 K to restore its adsorption capacity.

Reduction treatments combined with oxidation at 473 and 673 K have permitted a separated estimation of electronic and metal coverage contributions to the chemisorption loss in Rh/CeO_2 catalysts (SMSI effect). Both effects increase with the temperature and time of reduction; however, the electronic perturbation of the metal is favored in dynamic reductions. In samples reduced in static conditions, the contribution of the metal coverage becomes more relevant. In the first case, samples are more dehydroxylated that in the second case.

A comparative study of high-surface Rh/TiO_2 and Rh/CeO_2 catalysts showed that the electronic perturbation of Rh metal particles is higher in Rh/CeO_2 This observation results from the higher reducibility of CeO_2 with respect to TiO_2. On the other hand, migration of reduced species is more favorable in Rh/TiO_2 than in Rh/CeO_2. In low-surface textural-stabilized Rh/CeO_2 catalysts, diffusion of CeO_x species was only detected at temperatures near 1173 K; from this fact, the electronic effect is the preponderant contribution detected at 773 K.

Acknowledgment. Financial support provided by CICYT, Projects MAT-91-1080 and MAT-94-0835, is acknowledged. We thank Dr. J. P. Holgado for samples and Drs. J. M. Rojo, G. Munuera and J. Soria for helpful discussions. J.P.B. thanks the Ministerio de Educación y Ciencia of Spain for the fellowship.

References and Notes

(1) Trovarelli, A. *Catal. Rev.—Sci. Eng.* **1996**, *38*, 439.

(2) *Catalysis by Ceria and Related Materials*; Trovarelli, A., Ed.; Imperial College Press: London, 2002.

(3) Riguetto, B. A.; Damyanova, S.; Gouliev, G.; Marques, C. M. P.; Petrov, L.; Bueno, J. M. C. *J. Phys. Chem. B.* **2004**, *108*, 5349.

(4) Conesa, J. C.; Fernández-Gracía, M.; Martínez-Arias, A. *Catalysis by Ceria and Related Materials*; Trovarelli, A., Ed.; Imperial College Press: London, 2002; Chapter 5.

(5) Tauster, S. J.; Fung, S. C.; Garten, L. R. *J. Am. Chem. Soc.* **1978**, *100*, 170.

(6) Tauster, S. J. *Acc. Chem. Res.* **1987**, *20*, 389.

(7) Lamonier, C.; Wrobel, G.; Bonnelle, J.-P. *J. Mater. Chem.* **1994**, *4*, 1927.

(8) Lamonier, C.; Ponchel, A.; D'Huysser, L.; Jalowiecki-Duhamel, L. *Catal. Today* **1999**, *50*, 247.

(9) Bitter, J. H.; Cauqui, M. A.; Gatica, J. M.; Bernal, S.; Ramaker, D. E.; Koningesberger, D. C. *Stud. Surf. Sci. Catal.* **2000**, *130*, 3183.

(10) Eck, S.; Castellarini-Cudia, C.; Surnev, S.; Ramsey, M. G.; Netzer, F. P. *Surf. Sci.* **2002**, *520*, 173.

(11) Surnev, S.; Schoiswohl, J.; Kresse, G.; Ramsey, M. G.; Netzer, F. P. *Phys. Rev. Lett.* **2002**, *89*, 246101.

(12) Sadi, F.; Duprez, D.; Gérard, F.; Miloudi, A. *J. Catal.* **2003**, *213*, 226.

(13) Penner, S.; Wang, D.; Su, D. S.; Rupprechter, G.; Podloucky, R.; Schlögl, R.; Hayek, K. *Surf. Sci.* **2003**, *276*, 532.

(14) Penner, S.; Rupprechter, G.; Su, D. S.; Wang, D.; Tessadri, R.; Podloucky, R.; Schlögl, R.; Hayek, K. *Vacuum* **2003**, *71*, 71.

(15) Bernal, S.; Calvino, J. J.; Cauqui, M. A.; Gatica, J. M.; Larese, C.; Pérez Omil, J. A.; Pintado, J. M. *Catal. Today* **1999**, 175.

(16) Bernal, S.; Calvino, J. J.; Gatica, J. M.; López Cartes, C.; Pintado, J. M. *Catalysis by Ceria and Related Materials*; Trovarelli, A., Ed.; Imperial College Press: London, 2002; Chapter 4.

(17) Dulub, O.; Hebenstreit, W.; Diebold, U. *Phys. Rev. Lett.* **2000**, *84*, 3646.

(18) Werdinius, C.; Österlund, L.; Kasemo, B. *Langmuir* **2003**, *19*, 458.

(19) Österlund, L.; Kiebassa, S.; Werdinius, C.; Kassemo, B. *J. Catal*. **2003**, *215*, 94.

(20) Belzunegui, J. P.; Sanz, J.; Rojo, J. M. *J. Am. Chem. Soc*. **1990**, *112*, 4066.

(21) Belzunegui, J. P.; Sanz, J.; Rojo, J. M. *J. Am. Chem. Soc*. **1992**, *114*, 6749.

(22) Belzunegui, J. P.; Sanz, J. *J. Phys. Chem. B* **2003**, *107*, 11705.

(23) Force, C.; Belzunegui, J. P.; Sanz, J.; Martínez-Arias, A.; Soria, J. *J. Catal*. **2001**, *197*, 192.

(24) Sanz, J.; Rojo, J. M. *J. Phys. Chem*. **1985**, *89*, 4974.

(25) Rojo, J. M.; Belzunegui, J. P.; Sanz, J. *J. Phys. Chem*. **1994**, *98*, 13631.

(26) Cunningham, J.; O'Brien, S.; Sanz, J.; Rojo, J. M.; Soria, J. A.; Fierro, J. L. G. *J. Mol. Catal*. **1990**, *57*, 379.

(27) Cunningham, J.; Cullinane, D.; Sanz, J.; Rojo, J. M.; Soria, J. A.; Fierro, J. L. G. *J. Chem. Soc., Faraday Trans*. **1992**, *88*, 3233.

(28) Xu, J.; Overbury, S. H. *J. Catal*. **2004**, *222*, 167.

(29) Belzunegui, J. P.; Rojo, J. M.; Sanz, J. *J. Phys. Chem*. **1991**, *95*, 3463.